

Chapman University

Chapman University Digital Commons

Mathematics, Physics, and Computer Science
Faculty Articles and Research

Science and Technology Faculty Articles and
Research

10-26-2009

Continuous Phase Amplification with a Sagnac Interferometer

David J. Starling
University of Rochester

P. Ben Dixon
University of Rochester

Nathan S. Williams
University of Rochester

Andrew N. Jordan
University of Rochester

John C. Howell
Chapman University, johhowell@chapman.edu

Follow this and additional works at: https://digitalcommons.chapman.edu/scs_articles



Part of the [Optics Commons](#)

Recommended Citation

D. J. Starling, P. B. Dixon, NS Williams, A. N. Jordan, and J. C. Howell, *Continuous Phase Amplification with a Sagnac Interferometer*, Phys. Rev. A **82**(1), 011802. <https://doi.org/10.1103/PhysRevA.82.011802>

This Article is brought to you for free and open access by the Science and Technology Faculty Articles and Research at Chapman University Digital Commons. It has been accepted for inclusion in Mathematics, Physics, and Computer Science Faculty Articles and Research by an authorized administrator of Chapman University Digital Commons. For more information, please contact laughtin@chapman.edu.

Continuous Phase Amplification with a Sagnac Interferometer

Comments

This article was originally published in *Physical Review A*, volume 82, issue 1, in 2009. <https://doi.org/10.1103/PhysRevA.82.011802>

Copyright

American Physical Society

Continuous phase amplification with a Sagnac interferometer

David J. Starling, P. Ben Dixon, Nathan S. Williams, Andrew N. Jordan, and John C. Howell
Department of Physics and Astronomy, University of Rochester, Rochester, New York 14627, USA

(Received 26 October 2009; published 8 July 2010)

We describe a phase-amplification technique using a Sagnac interferometer. We monitor the relative phase between two paths of a precisely misaligned interferometer by measuring the average position of a split-Gaussian mode in the dark port. Although we monitor only the dark port, we show that the signal varies linearly with phase and that we can obtain similar sensitivity to balanced homodyne detection. We derive the source of the amplification using classical wave optics.

DOI: [10.1103/PhysRevA.82.011802](https://doi.org/10.1103/PhysRevA.82.011802)

PACS number(s): 42.25.Hz, 42.60.Mi, 42.87.Bg, 07.60.Ly

Introduction. Phase measurements using coherent light sources continue to be of great interest in classical optics [1–5]. Not surprisingly, many advances in phase measurement techniques have been made since the introduction of the laser. For instance, Caves emphasized how the signal-to-noise ratio (SNR) of a phase measurement can be improved by using a squeezed vacuum state in the dark input port of an interferometer [6]. Related advances in this area include the use of other nonclassical states of light such as Fock states [7] or the use of phase-estimation techniques [8] which approach the Heisenberg limit in phase sensitivity [9]. Unfortunately, these states of light tend to be weak and very sensitive to losses, in effect reducing the SNR of a phase measurement. As a result, the use of coherent light sources has dominated the field of precision metrology [10,11] where the phase sensitivity scales as $1/\sqrt{N}$ rad, where N is the average number of photons used in the measurement.

In this paper, we show that it is possible to make a measurement of phase with the same SNR as balanced homodyne detection, yet only the light in the dark port is measured. We use a coherent light source with a split detector in a Sagnac interferometer and show that the signal of a phase measurement is amplified. Due to the large reduction of the intensity at the detector, we can in principle use a low-cost detector with a low saturation intensity and still obtain significantly higher phase sensitivity when compared to that obtained using a balanced homodyne detector with the same total incident intensity. This method may improve the sensitivity of high-power balanced homodyne phase measurements.

We derive our results using a classical wave description but point out here that a quantum treatment which uses a similar formalism to that presented in Refs. [11,12] is also valid.

Theory. Consider a coherent light source with a Gaussian amplitude profile entering the input port of a Sagnac interferometer, as shown in Fig. 1. The interferometer is purposely misaligned using a piezo-actuated mirror such that the two paths experience opposite deflections. The transverse momentum shift imparted by the mirror is labeled as k . A relative phase shift ϕ can be induced between the two light paths (clockwise and counterclockwise) in the interferometer.

We model the electric field propagation using standard matrix methods in the paraxial approximation. We can then write the input electric field amplitude as

$$\mathbf{E}_{\text{in}} = (E_0 e^{-x^2/4\sigma^2} \mathbf{0})^T, \quad (1)$$

where σ is defined as the Gaussian beam radius. The first position in the column vector denotes port 1 (see Fig. 1) of the beam splitter and the second position denotes port 2 (with no input electric field). We assume that the beam is large enough so that the entire Rayleigh range fits within the interferometer. The matrix representation for the 50:50 beam splitter is given by

$$\mathbf{B} = \frac{1}{\sqrt{2}} \begin{pmatrix} 1 & i \\ i & 1 \end{pmatrix}, \quad (2)$$

where column and row one correspond to port 4 (counterclockwise) and column and row two correspond to port 3 (clockwise). We now define a matrix that gives both an opposite momentum shift k and a relative phase shift ϕ between the two light paths:

$$\mathbf{M} = \begin{pmatrix} e^{i(-kx+\phi/2)} & 0 \\ 0 & e^{-i(-kx+\phi/2)} \end{pmatrix}. \quad (3)$$

We assume a short propagation distance and a large beam radius σ and thus ignore any divergence of the beam. Therefore, the exiting electric field amplitude after propagation is represented by the matrix combination $(\mathbf{BMB})\mathbf{E}_{\text{in}}$,

$$\mathbf{E}_{\text{out}} = i E_0 e^{-x^2/4\sigma^2} \begin{pmatrix} -\sin(kx - \phi/2) \\ \cos(kx - \phi/2) \end{pmatrix}, \quad (4)$$

where the first position now corresponds to port 2 (the dark port) and the second position corresponds to port 1 (the bright port).

For a balanced homodyne detection scheme, we take $k = 0$ and $\phi \rightarrow \pi/2 + \phi$ and subtract the integrated intensity of both output ports. After normalizing by the total power, we obtain the unitless homodyne signal

$$\Delta_h = \sin \phi \approx \phi. \quad (5)$$

Thus, we see that by balancing the interferometer, we are measuring the signal along the linear part of the sine curve for small phase shifts.

In contrast, if we consider a small transverse momentum shift ($k\sigma < 1$) and monitor only the dark port, given by the first element in the \mathbf{E}_{out} vector, we find that

$$E_{\text{out}}^{(d)} \approx A \left[\frac{x}{\sigma} - \frac{\tan(\phi/2)}{k\sigma} \right] \exp[-x^2/4\sigma^2], \quad (6)$$

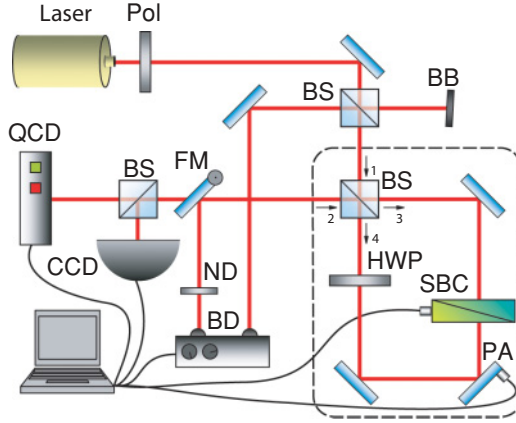


FIG. 1. (Color online) Experimental setup. A coherent light source passes through a polarizer (Pol), producing horizontally polarized light before passing through the first 50:50 beam splitter (BS). Half of the light strikes a beam block (BB) and is thrown out. The beam then enters the Sagnac interferometer via the second BS. One of the mirrors of the interferometer is controlled by a piezo actuator (PA) to precisely control the relative transverse momentum shift k . We use a half-wave plate (HWP) and a piezo-actuated Soleil-Babinet compensator (SBC) to produce a relative phase shift between the two light paths. During split detection, we monitor the dark port using another BS that splits the light between a quad-cell detector (QCD) and a charge-coupled-device camera (CCD). During balanced homodyne detection, the interferometer is balanced and the flip mirror (FM) is turned up, sending both bright (1) and dark (2) ports into the balance detector (BD). We use a neutral density filter (ND) in the dark port to correct for the light lost at the first BS.

where $A = -iE_0k\sigma \cos(\phi/2)$. The intensity at the dark port is then given by

$$I_d(x) = P_{ps}I_0 \left[\frac{x}{\sigma} - \frac{\tan(\phi/2)}{k\sigma} \right]^2 \exp[-x^2/2\sigma^2], \quad (7)$$

where P_{ps} is the attenuation (postselection probability) of the measured output beam given by

$$P_{ps} = |k\sigma \cos(\phi/2)|^2, \quad (8)$$

and I_0 is the maximum input intensity density. Aside from the attenuation factor P_{ps} , $I_d(x)$ is normalized to the input for vanishingly small ϕ . Equation (7) is plotted in Fig. 2.

The average position of the postselected beam given by Eq. (7) is simply

$$\langle x \rangle \approx -\phi/k. \quad (9)$$

We interpret Eq. (9) as an amplification of the small phase shift ϕ by the mirror's momentum kick k .

Instead of measuring the average position, one can use a split-detection method by subtracting the integrated intensity on the left side of the detector from the integrated intensity on the right side of the detector. This detection method is well suited to the split-Gaussian beam and results in a split-detection signal which, if normalized by the total power striking the detector, is proportional to the average position. This quantity is given by

$$\Delta_s \approx -\sqrt{\frac{2}{\pi}} \frac{\phi}{k\sigma} \approx \sqrt{\frac{2}{\pi\sigma^2}} \langle x \rangle. \quad (10)$$

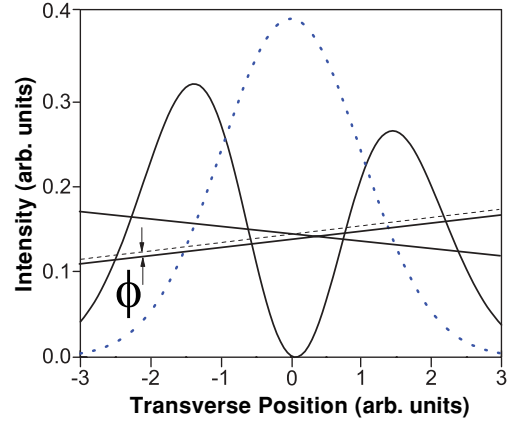


FIG. 2. (Color online) Postselected intensity distribution. The dotted (blue) curve is the single-mode input profile of the beam in the interferometer. The solid (black) curve is the postselected split-Gaussian mode produced by the misalignment of the interferometer and a slight relative phase shift between the two light paths. The solid lines represent the tilted wave fronts in the two paths of the interferometer when they combine at the BS, one that is delayed relative to the other, producing an asymmetric split-Gaussian (shown). The dashed line represents a wave front with the same tilt but zero relative phase delay, which would result in a symmetric split-Gaussian (not shown).

Despite the large amplification of the average position measurement of the postselected intensity, the SNR is essentially the same for a balanced homodyne measurement of phase using the same *input power*. The SNR of a phase measurement using balanced homodyne or split detection can be expressed explicitly as $\mathcal{R}_{h,s} = \Delta_{h,s} \sqrt{N_d}$, where N_d is the number of photons *striking the detector*. In the case of homodyne detection, $N_d = N$. In the case of split detection, the postselection reduces this quantity to $N_d = N|k\sigma \cos(\phi/2)|^2$. Therefore, \mathcal{R}_h and \mathcal{R}_s are identical for small ϕ , except for an overall constant factor of $\sqrt{2/\pi}$. This reduces the SNR of the split-detection method by approximately 20%. It is also interesting to note that the SNR is independent of k . Thus, we can in principle reduce k (and P_{ps}) arbitrarily, allowing us to increase the input power and therefore N , ultimately improving the measurement sensitivity arbitrarily while using the same detector.

Experiment. In the present experiment (see Fig. 1), the coherent light beam was created using an external cavity diode laser tuned approximately to 795 nm. The beam was coupled into single-mode fiber and then launched to produce a single-mode Gaussian profile. The light was collimated with a radius of $\sigma \approx 775 \mu\text{m}$ and the continuous wave power ranged from 0.5 to 1 mW. The Sagnac, composed of a 50:50 beam splitter and three mirrors, was rectangular. We used two configurations for the geometry of the interferometer, one with dimensions 39×8 cm (large) and another with dimensions 11×8 cm (small). The beam profile and position of the postselected photons were measured using a quad-cell detector (QCD, New Focus Model 2921) functioning as a split detector and a CCD camera (Newport Model LBP-2-USB). During balanced homodyne detection, the signal was measured using a Nirvana balance detector (BD, New Focus Model 2007). The quantum efficiency of the BD was about 81%,

whereas the quantum efficiency of the QCD was 75%. The QCD was also equipped with a protective neutral density filter with 50% transmissivity. The outputs from the QCD and the BD were fed into two low-noise preamplifiers with frequency filters (Stanford Research Systems Model SR560) in series.

We used a half-wave plate (HWP) with a piezo-actuated Soleil-Babinet compensator (SBC) inside the Sagnac interferometer to induce a relative phase shift. The HWP was oriented such that the horizontally polarized input light was rotated to vertically polarized light. The SBC was oriented such that the fast axis was vertical and the slow axis was horizontal. The two light paths in the interferometer encountered these optical elements in opposite order, allowing for a known, tunable phase difference between them. The piezo actuator in the SBC, which moved approximately 100 pm/mV, imparted a relative phase shift of $22 \pm 0.9 \mu\text{rad}/\text{V}$.

Using the large configuration, with 0.5 mW of input power, the piezo actuator in the SBC was driven with a 20-V peak to peak sine wave at 634 Hz, corresponding to a relative phase shift of $440 \mu\text{rad}$. The normalized split-detection signal Δ_s (factoring in an offset from spurious light hitting the detector) was measured while the transverse momentum shift k was varied using the piezo-actuated mirror. After scaling Δ_s by the appropriate factor given in Eq. (10), the results were plotted in Fig. 3. The theory line, which corresponds to a relative phase shift of $440 \mu\text{rad}$, is drawn along with the data. We see good agreement of the data with theory, with a clear inverse dependence of $\langle x \rangle$ on k . However, it should be noted that a determination of k for this fit requires calibration, which in practice is quite simple.

We then compared this split-detection method of phase measurement to a balanced homodyne measurement. We used the small configuration with $625 \mu\text{W}$ of (effective) continuous wave input power—taking into account various attenuators—and varied the driving voltage to the piezo actuator in the SBC. The low-pass filter limits the laser noise to the 10% to 90% rise time of a 1-kHz sine wave ($300 \mu\text{s}$). We take this limit as our integration time to determine the number of 795-nm photons used in each measurement. We measured the SNR of a phase

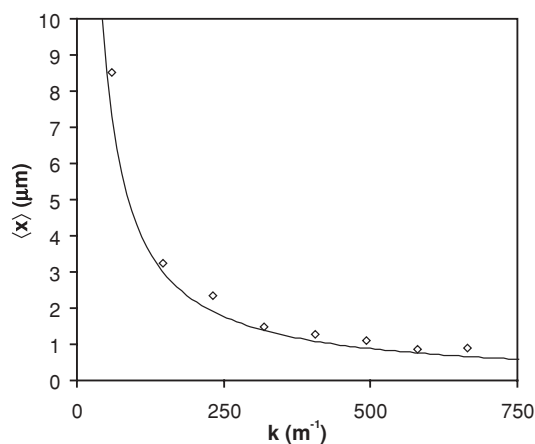


FIG. 3. Dependence on transverse momentum. The transverse momentum shift imparted by the piezo-actuated mirror was varied and the split-detection signal was measured using the QCD. The solid line is the theory curve from Eq. (9) using the expected phase shift.

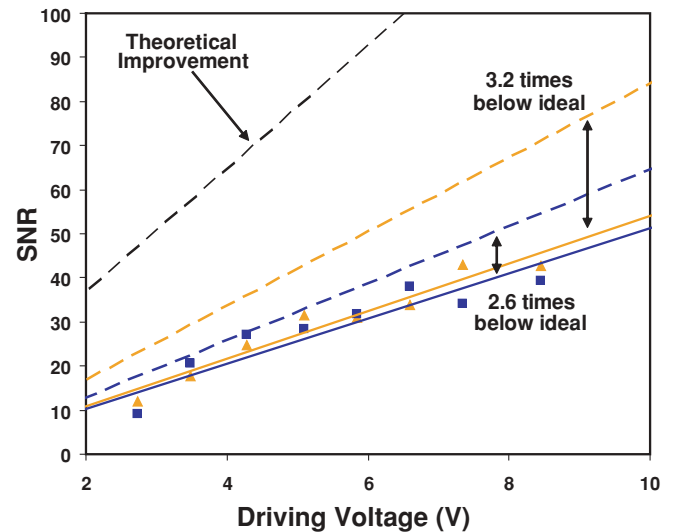


FIG. 4. (Color online) Experimental comparison of split-detection to balanced homodyne. We vary the driving voltage applied to the piezo actuator and measure the SNR using balanced homodyne detection (orange triangles) and the split-detection method (blue squares). The input power to the interferometer is approximately the same for both methods. Linear fits to the data (solid lines) show that these two methods have essentially the same sensitivity. The ideal quantum limited SNR (factoring in the quantum efficiency of each detector) is plotted using the lower, dashed blue line (split-detection) or the middle, dashed orange line (balanced homodyne detection). The higher, dashed black line illustrates the theoretical (\sqrt{N}) improvement of the split-detection method assuming that an equal number of photons are incident on both the split-detector and the balance detector.

measurement (see Fig. 4) using the same method as Ref. [12] and found that the SNR of our homodyne measurement was on average 3.2 times below an ideal quantum limited system. The SNR of our split-detection method was on average 2.6 times below an ideal quantum limited system. We take into account the quantum efficiency of each detector so that the number of photons used with each technique is the same for these two values, yet we ignore any contribution of dark current, thermal, or mechanical noise to the expected SNR.

Importantly, the SNR resulting from both measurement techniques is approximately the same. However, the split-detection method for this data had only about 15% of the input light incident on the detector. Thus, for diodes with the same saturation intensity, it is possible to use almost seven times more input power with this configuration, resulting in a SNR about 2.6 times higher (the black, dashed line in Fig. 4). The improvement of the SNR by taking advantage of the attenuation before the detector has no theoretical limit and is only limited in practice by phase front distortions and back-reflections off of optical surfaces which degrade the fidelity of the interference. Using commercially available equipment and one day of integration time, subpicoradian sensitivity is possible even with a low-saturation intensity split detector.

Conclusion. In summary, we have shown that the measurement of a relative phase shift between two paths in an interferometer can be measured and amplified using a split-detection method. We note that, although a Sagnac was used in

this experiment, the same results apply to other interferometers (e.g., Michelson). Additionally, this method is comparable to the sensitivity achievable using balanced homodyne techniques, yet only the dark port of the interferometer is measured. The split detector can have a low saturation intensity owing to the large attenuation. In fact, the higher the attenuation, the larger the amplification of the split-detection signal. Last, although we have described this experiment classically, we note that a quantum treatment is equally valid.

We believe that this technique is a robust, low-cost alternative to balanced homodyne phase detection and may have applications in a number of fields, for example, magnetometry (using nonlinear magneto-optical rotation) or rotation sensing.

This research was supported by US Army Research Office Grant No. W911NF-09-0-01417 and DARPA Expansion Grant No. N00014-08-1-120.

-
- [1] K.-X. Sun *et al.*, *Opt. Lett.* **22**, 1359 (1997).
[2] R. Erlandsson *et al.*, *J. Vac. Sci. Technol. A* **6**, 266 (1988).
[3] E. J. Post, *Rev. Mod. Phys.* **39**, 475 (1967).
[4] J. Schmitt, *IEEE J. Sel. Top. Quantum Electron.* **5**, 1205 (1999).
[5] A. Wehr and U. Lohr, *ISPRS J. Photogramm. Remote Sens.* **54**, 68 (1999).
[6] C. M. Caves, *Phys. Rev. D* **23**, 1693 (1981).
[7] M. J. Holland and K. Burnett, *Phys. Rev. Lett.* **71**, 1355 (1993).
[8] B. L. Higgins *et al.*, *New J. Phys.* **11**, 073023 (2009).
[9] Z. Y. Ou, *Phys. Rev. A* **55**, 2598 (1997).
[10] A. Abramovici *et al.*, *Science* **256**, 325 (1992).
[11] P. B. Dixon, D. J. Starling, A. N. Jordan, and J. C. Howell, *Phys. Rev. Lett.* **102**, 173601 (2009).
[12] D. J. Starling, P. B. Dixon, A. N. Jordan, and J. C. Howell, *Phys. Rev. A* **80**, 041803(R) (2009).